

Article

An Extract from Shrimp Processing By-Products Protects SH-SY5Y Cells from Neurotoxicity Induced by A β _{25–35}

Yongping Zhang ^{1,2}, Guangling Jiao ^{3,4}, Cai Song ^{1,2,5,*}, Shelly Gu ², Richard E. Brown ², Junzeng Zhang ⁴, Pingcheng Zhang ², Jacques Gagnon ³, Steven Locke ⁶, Roumiana Stefanova ⁴, Claude Pelletier ³, Yi Zhang ¹ and Hongyu Lu ¹

¹ Research Institute for Marine Drugs and Nutrition, College of Food Science and Technology, Guangdong Ocean University, Zhanjiang 524088, China; zhangyp2015@163.com (Y.Z.); hubeizhangyi@163.com (Y.Z.); irislyh@126.com (H.L.)

² Department of Psychology and Neuroscience, Dalhousie University, Halifax, NS B3H 4R2, Canada; xiaomei.gu@dal.ca (S.G.); Richard.Brown@dal.ca (R.E.B.); pczhang2000@yahoo.com (P.Z.)

³ Coastal Zones Research Institute Inc., 232B, avenue de l'Église, Shippagan, NB E8S 1J2, Canada; sebrina2006@gmail.com (G.J.); jacques.gagnon@umoncton.ca (J.G.); Claude.pelletier@umoncton.ca (C.P.)

⁴ Aquatic and Crop Resource Development, National Research Council of Canada, 1411 Oxford Street, Halifax, NS B3H 3Z1, Canada; Junzeng.Zhang@nrc-cnrc.gc.ca (J.Z.); Roumiana.Stefanova@nrc-cnrc.gc.ca (R.S.)

⁵ Graduate Institute of Neural and Cognitive Sciences, China Medical University Hospital, Taichung 40402, Taiwan

⁶ Aquatic and Crop Resource Development, National Research Council of Canada, 550 University Avenue, Charlottetown, PE C1A 4P3, Canada; Steven.Locke@nrc-cnrc.gc.ca

* Correspondence: cai.song@dal.ca; Tel.: +86-759-239-6047

Academic Editors: Rosário Domingues, Ricardo Calado and Pedro Domingues

Received: 8 December 2016; Accepted: 15 March 2017; Published: 22 March 2017

Abstract: Increased evidence suggests that marine unsaturated fatty acids (FAs) can protect neurons from amyloid- β (A β)-induced neurodegeneration. Nuclear magnetic resonance (NMR), high performance liquid chromatography (HPLC) and gas chromatography (GC) assays showed that the acetone extract 4-2A obtained from shrimp *Pandalus borealis* industry processing wastes contained 67.19% monounsaturated FAs and 16.84% polyunsaturated FAs. The present study evaluated the anti-oxidative and anti-inflammatory effects of 4-2A in A β _{25–35}-insulted differentiated SH-SY5Y cells. Cell viability and cytotoxicity were measured by using 3-(4,5-Dimethylthiazol-2-yl)-2,5-diphenyltetrazolium bromide (MTT) and lactate dehydrogenase (LDH) assays. Quantitative PCR and Western blotting were used to study the expression of neurotrophins, pro-inflammatory cytokines and apoptosis-related genes. Administration of 20 μ M A β _{25–35} significantly reduced SH-SY5Y cell viability, the expression of nerve growth factor (NGF) and its tyrosine kinase TrkA receptor, as well as the level of glutathione, while increased reactive oxygen species (ROS), nitric oxide, tumor necrosis factor (TNF)- α , brain derived neurotrophic factor (BDNF) and its TrkB receptor. A β _{25–35} also increased the Bax/Bcl-2 ratio and Caspase-3 expression. Treatment with 4-2A significantly attenuated the A β _{25–35}-induced changes in cell viability, ROS, GSH, NGF, TrkA, TNF- α , the Bax/Bcl-2 ratio and Caspase-3, except for nitric oxide, BDNF and TrkB. In conclusion, 4-2A effectively protected SH-SY5Y cells against A β -induced neuronal apoptosis/death by suppressing inflammation and oxidative stress and up-regulating NGF and TrkA expression.

Keywords: Acetone extract from shrimp processing by-product (4-2A); polyunsaturated fatty acids; A β _{25–35}; human neuroblastoma cell (SH-SY5Y); neuroprotection; Alzheimer's disease (AD)

1. Introduction

The neurodegenerative process in Alzheimer's disease (AD) is associated with progressive accumulation of intracellular and extracellular neurotoxic amyloid- β ($A\beta$) oligomers in the brain [1–3]. Excessive $A\beta$ -deposition may induce AD through oxidative stress and neuroinflammation. Amyloid-beta oligomers can activate microglia in vitro and in vivo [4], resulting in the production and release of reactive oxygen species (ROS) and pro-inflammatory cytokines such as tumor necrosis factor (TNF)- α , both of which can cause neural degeneration. Elevated levels of ROS interfere with the actions of many key molecules including enzymes, membrane lipids and DNA, which leads to cell apoptosis or death [5,6]. Increased pro-inflammatory cytokine release may stimulate neurons to produce increased amounts of $A\beta$ oligomers and cause neuronal dysfunction and apoptosis [7,8]. Another hallmark of AD is decreased neurogenesis due to the dysfunction in neurotrophic signaling mechanisms [9]. In particular, nerve growth factor (NGF) and brain-derived neurotrophic factor (BDNF) and their receptors in the brain are disrupted. Reduced BDNF expression in the brain is a common feature of AD and cognitive dysfunction [10]. In addition, $A\beta$ peptides are able to interfere with BDNF signal transduction pathways involved in neuronal survival and synaptic plasticity, hampering the transmission of neurotrophic responses [11].

Because the etiology of AD remain unknown, treatments that target AD are ineffective and often cause severe side-effects [12]. Most neurodegenerative diseases, including AD, are irreversible because the failure of neurogenesis and the increase in neuron death occurs before the clinical symptoms appear [13]. Thus, much effort is directed towards the discovery of neural pathways and their molecular mechanism that can be targeted by novel therapeutics to prevent AD. Natural substances with anti-oxidative and/or anti-inflammatory activity could provide effective treatments for the prevention of AD.

In the past decade, many studies have demonstrated that unsaturated fatty acids of marine origin, such as omega (*n*)-3 and *n*-9 fatty acids, could play a beneficial role in brain functions. Our previous studies have highlighted the effectiveness of dietary *n*-3 polyunsaturated fatty acids (PUFAs) as a potential treatment strategy for affective diseases [14,15]. Recent studies have demonstrated that eicosapentaenoic acid (EPA) and docosahexaenoic acid (DHA) possess neuroprotective properties because of their anti-oxidant and anti-inflammatory functions [14–16]. There are also data showing neuroprotective potential of monounsaturated fatty acids (MUFAs). For example, oleic acid, which belongs to *n*-9 MUFAs, has been found to modulate mitochondrial dysfunction, insulin resistance and inflammatory signaling [17–19] and act as neurotrophic factors for neurons [20]. Palmitoleic acid, a naturally occurring 16-carbon *n*-7 MUFA, and one of the most abundant fatty acids in the serum and tissues, was considered to be a lipokine and has been found to benefit some physiological function, such as regulating cell proliferation, and decreasing the expression of pro-inflammatory mediators and adipokines [21–23].

Tchoukanova and Benoit [24] developed a method to recover organic solids and oils from marine by-products. Using this method, shrimp oil was produced and found to be rich in long-chain unsaturated fatty acids [25]. The solid residue may also contain nutritional and bioactive ingredients that can be exploited. In the present study, an acetone extract 4-2A obtained from the solid phase was found to be rich in *n*-3 and *n*-9 unsaturated fatty acids. Because of the above mentioned neuroprotective function of unsaturated fatty acids, the present study aimed to determine whether the 4-2A extract from shrimp by-products would protect neurons from $A\beta$ -induced neurotoxicity via its regulation of neurotrophic function, anti-inflammatory and anti-oxidative effects. To carry out this experiment, a cellular model of AD was set up using $A\beta_{25-35}$ -insulted differentiated SH-SY5Y cells. Following this, the effects of 4-2A on $A\beta_{25-35}$ -induced changes in cell viability, oxidative stress (ROS, NO, and GSH) and neurotrophins (NGF, BDNF and their TrkA and TrkB receptors) were measured. Since TNF- α is a key "pro-neuropathic" cytokine [26] and can activate a pro-apoptotic factor JNK pathway and trigger cellular death signaling [27], TNF- α expression was measured to test 4-2A anti-inflammatory effect in the present study. Then, the ability of 4-2A to regulate the expression of apoptosis-related genes (Bcl-2,

Bax and Caspase-3) in the model was explored. The experimental design and content is presented in Figure 1.

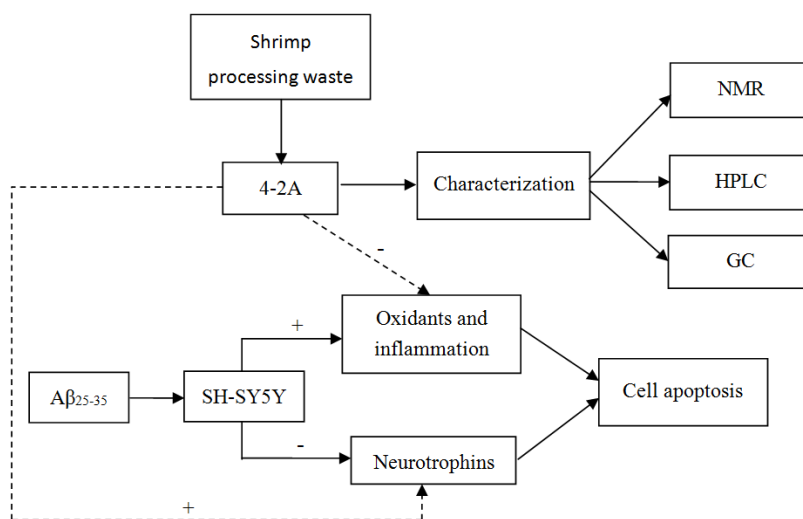


Figure 1. Experimental design and contents. NMR: Nuclear Magnetic Resonance; HPLC: High Performance Liquid Chromatography; GC: Gas Chromatograph. “+”: strengthening; “−”: weakening.

2. Results

2.1. Characterization of Shrimp Extract 4-2A

Reddish and oily sample 4-2A was extracted from the solid residue of shrimp processing waste using acetone and yielded 2.55% of original dry mass. Both $^1\text{H-NMR}$ and $^{13}\text{C-NMR}$ spectra indicated that this shrimp extract was rich in lipids. The detailed assignments of the most common proton and carbon signals are shown in Figure 2. They have been compiled in the online resources of AOCS Lipid Library by a wide range of fatty compounds [28]. The spectra ranging from 0 to 6 ppm in the $^1\text{H-NMR}$ spectrum covered the proton chemical shifts of most lipids (Figure 2A). To be noted, the signals around 2.8 ppm indicated the presence of methylenes between two double bonds $-\text{CH}=\text{CH}-\text{CH}_2-\text{CH}=\text{CH}-$, a typical feature of polyunsaturated fatty acids. The shifts at 0.93–1.01 ppm suggested the protons of ω -3 terminal methyl groups. The intensity of these signals indicated that 4-2A contained relatively high level of ω -3 PUFAs. The chemical shifts between 3.5 and 4.0 ppm showed the presence of small amount of monoglycerides.

In the $^{13}\text{C-NMR}$ spectrum (Figure 2B), the chemical shifts at 180.3 ppm indicated the carbons of $\text{C}=\text{O}$ groups. The shifts around 130 ppm showed the two olefinic carbon atoms of double bonds. The carbons of the terminal methyl groups of lipids were identified by the chemical shifts at 15.3–15.6 ppm. Collectively, the major components of 4-2A were identified by NMR as lipids containing large amount of unsaturated fatty acids.

Lipid standards were subjected on HPLC to qualify the separations. As indicated in Figure 3, the major components of 4-2A are free fatty acids and monoglycerides with elution window from 16 min to 36 min by charged aerosol detector (CAD). Based on the chromatogram, this extract does not contain much triglycerides and phospholipids. This is consistent with the result obtained from NMR analyses.

In order to understand the fatty acids profiles in this shrimp extract, the total fatty acids were released from 4-2A and analyzed on GC instrument. As a result shown in Table 1, the major FAME profiles of 4-2A was 18:1*n*-9 (20.65%), 16:1*n*-7 (14.75%), 22:1*n*-7 (11.04%), 20:5*n*-3 (8.45%), 20:1*n*-9 (7.97%), 18:1*n*-7 (7.07%), 16:0 (6.56%) and 22:6*n*-3 (6.54%). Most fatty acids (over 93%) are unsaturated, including 67.19% of monounsaturated fatty acids (MUFAs) and 16.84% of polyunsaturated fatty acids (PUFAs). To be mentioned, 4-2A contains 14.99% of omega-3 fatty acids (20:5*n*-3, Eicosapentaenoic acid, EPA and 22:6*n*-3, Docosahexaenoic acid, DHA).

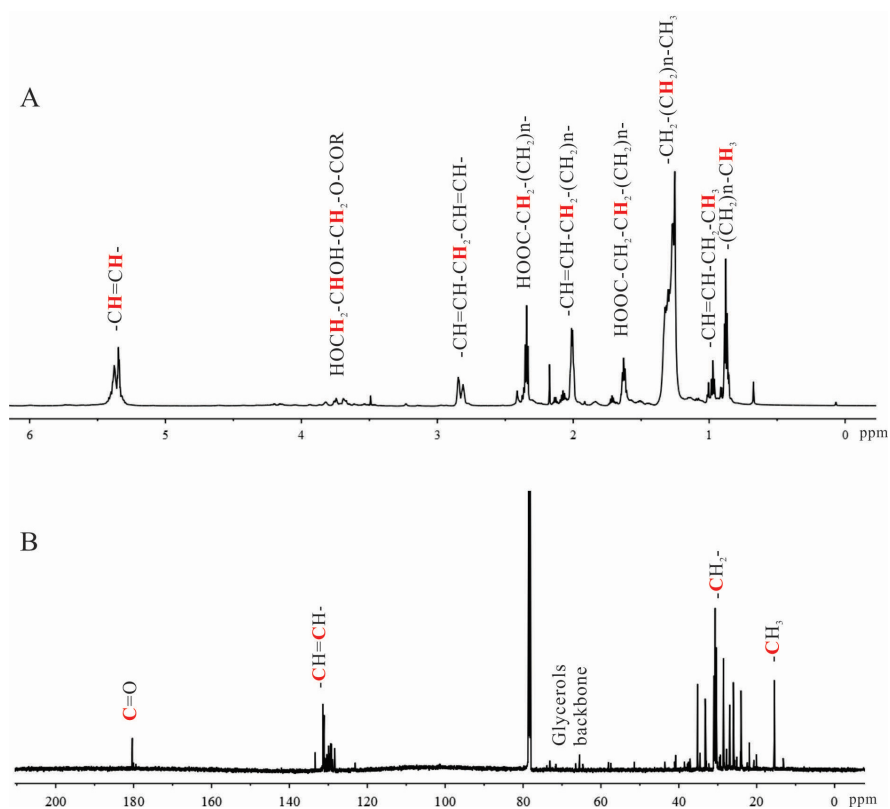


Figure 2. Characterization of 4-2A by NMR: (A) ^1H -NMR spectrum ($n \geq 1$); and (B) ^{13}C -NMR spectrum.

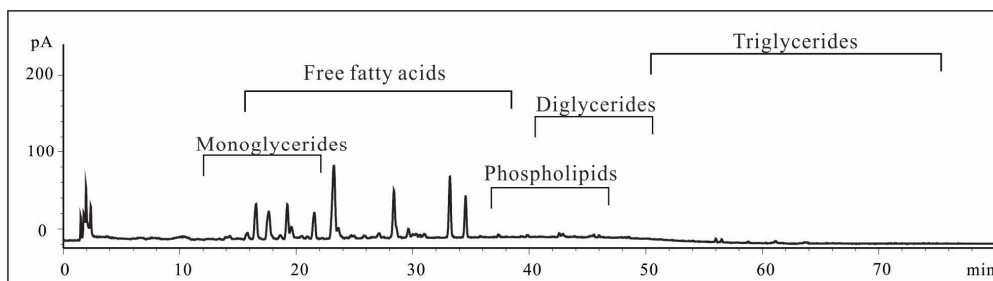


Figure 3. Characterization of 4-2A by HPLC with CAD detector.

Table 1. Major fatty acid methylated esters (FAME) profiles of 4-2A by GC analysis.

FAME	Intensity (%)	Stdev ($n = 4$, %)
14:0	2.10	0.25
16:0	6.56	0.58
18:0	0.70	0.08
16:1 <i>n</i> -7	14.75	0.21
18:1 <i>n</i> -5	0.77	0.16
18:1 <i>n</i> -7	7.07	0.31
18:1 <i>n</i> -9	20.65	2.62
20:1 <i>n</i> -7	1.08	0.03
20:1 <i>n</i> -9	7.97	0.97
20:1 <i>n</i> -11	1.95	0.01
22:1 <i>n</i> -7	11.04	0.24
22:1 <i>n</i> -9	1.91	0.78
18:2 <i>n</i> -6	0.86	0.10
20:4 <i>n</i> -6	0.99	0.12

Table 1. Cont.

FAME	Intensity (%)	Stdev (n = 4, %)
20:5n-3	8.45	0.83
22:6n-3	6.54	1.02
Total	93.39	
Saturated	9.36	
Monounsaturated	67.19	
Polyunsaturated	16.84	
Omega-3	14.99	
Omega-6	1.85	
Omega-7	33.94	
Omega-9	30.53	

In brief, the acetone extract 4-2A obtained from shrimp processing wastes was identified by NMR, HPLC and GC to contain mainly unsaturated free fatty acids and monoglycerides, including ω -3 PUFAs.

2.2. $A\beta_{25-35}$ -Induced Decrease in Neuronal Cell Viability Was Ameliorated by 4-2A

The cell morphology of differentiated SH-SY5Y cells is more like the classic neuron-like cells with long synapse compared to undifferentiated cells (Figure 4). As detected by 3-(4,5-Dimethylthiazol-2-yl)-2,5-diphenyltetrazolium bromide (MTT) method, $A\beta_{25-35}$ significantly decreased cell viability of differentiated SH-SY5Y cells in a time- and dose-dependent manner, such as at 15 μ M for 12 h ($p > 0.05$), 24 h ($p < 0.05$) and 48 h ($p < 0.01$); and at 10 μ M ($p > 0.05$), 15 μ M ($p < 0.05$) and 20 μ M ($p < 0.01$) for 24 h (Figure 5A). 4-2A treatment (1–20 μ g/mL) alone did not exert any significant influence on the survival rate of SH-SY5Y cells, though 40 μ g/mL of 4-2A slightly decreased the cell viability ($p > 0.05$) (Figure 5B). However, pretreated with different concentrations of 4-2A markedly attenuated the reduction of cell viability caused by $A\beta_{25-35}$ in a dose-dependent manner at 1 ($p > 0.05$), 5 ($p < 0.05$), and 10–20 μ g/mL (all $p < 0.01$) (Figure 5C). The protective role of 4-2A against $A\beta_{25-35}$ -induced insults in SH-SY5Y cells was further confirmed by lactate dehydrogenase (LDH) release assay (Figure 5D), which is an index of cell death. Combining the results from above assays, we could safely draw the conclusion that 4-2A could effectively protect the differentiated SH-SY5Y cells from $A\beta_{25-35}$ -induced cellular damage.

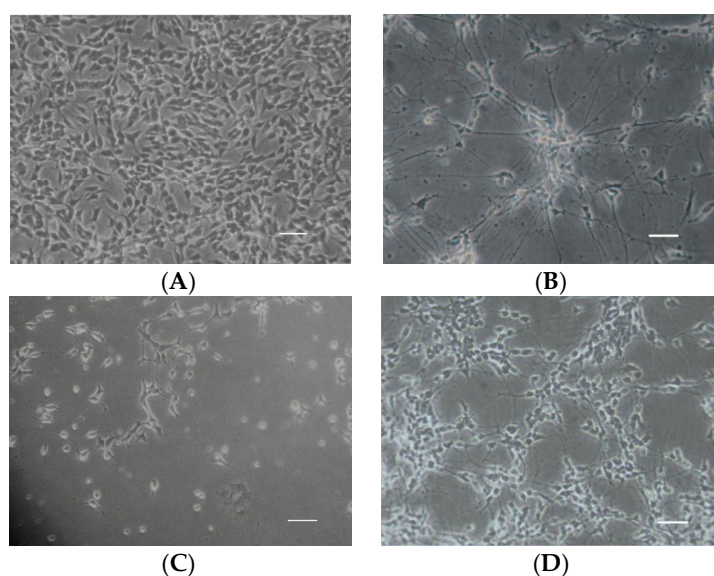


Figure 4. Cell morphology of undifferentiated SH-SY5Y cells (A); differentiated SH-SY5Y cells (B); differentiated SH-SY5Y cells insulted by $A\beta_{25-35}$ (C); and differentiated SH-SY5Y cells treated with 4-2A and $A\beta_{25-35}$ (D). Scale bar = 50 μ m.

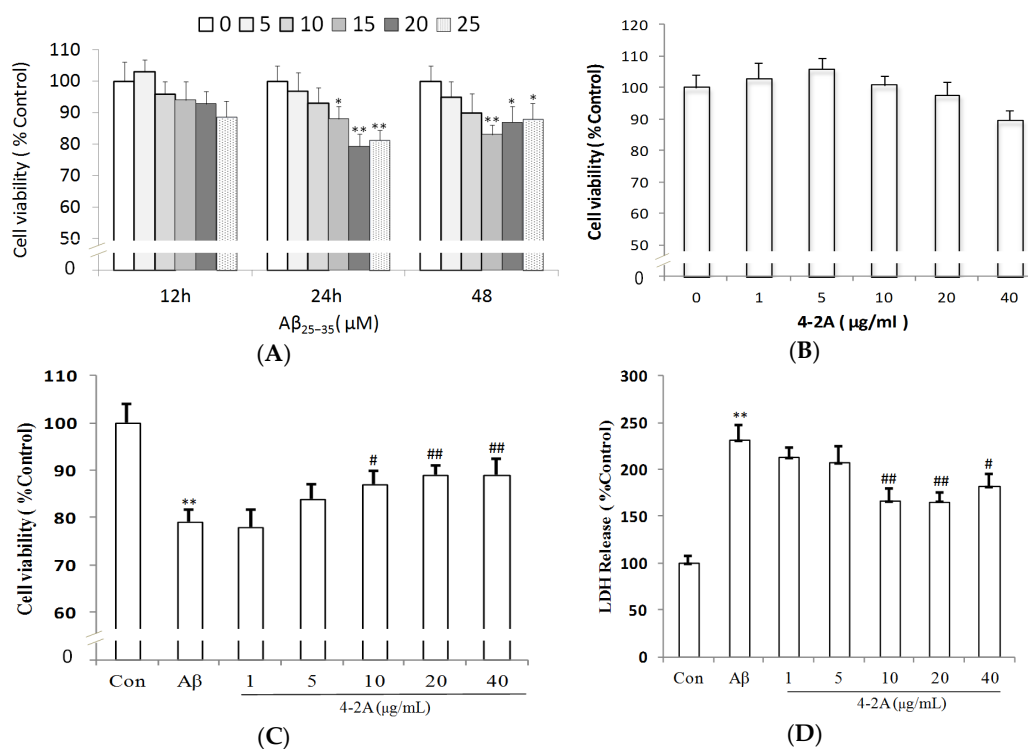


Figure 5. Cell viability and Cytotoxicity: (A) Treatment of Aβ₂₅₋₃₅ at various doses for 12 h, 24 h and 48 h; (B) cells treated with 4-2A at indicated doses for 24 h; (C) changes in cell survival rate after the treatment with 20 μM Aβ₂₅₋₃₅ for 24 h in the absence or presence of 4-2A at indicated doses; and (D) changes in lactate dehydrogenase (LDH) release after the treatment with 20 μM Aβ₂₅₋₃₅ for 24 h in the absence or presence of 4-2A at indicated doses. Data represent mean ± SEM of three separate experiments ($n = 4$ in each experiment) and three mean values from independent experiment were used for statistics. * $p < 0.05$, ** $p < 0.01$ vs. control group; # $p < 0.05$, ## $p < 0.01$ vs. Aβ₂₅₋₃₅ group.

2.3. Treatment with 4-2A Attenuated the Changes in ROS, Nitric Oxide (NO) and Glutathione (GSH) Level Induced by Aβ₂₅₋₃₅

Figure 6A illustrated that Aβ₂₅₋₃₅ markedly increased ROS fluorescence when compared to control group ($p < 0.01$). However, cells pretreated with 4-2A (10 μg/mL) showed a partial decrease in mean fluorescence intensities by about 23% when compared to Aβ₂₅₋₃₅-insulted group ($p < 0.05$). As shown in Figure 6C, a significant increase of about 44.42% in the level of nitrate was observed when the cells were treated with Aβ₂₅₋₃₅ alone ($p < 0.05$), while 4-2A pre-treatment could not attenuate the Aβ₂₅₋₃₅-induced change in NO concentration. The results shown in Figure 6C indicate a marked reduction in the GSH content of the Aβ₂₅₋₃₅ insulted cells ($p < 0.05$), and 4-2A pre-treatment could completely restore this reduction ($p < 0.01$).

2.4. Treatment with 4-2A Attenuated the Aβ₂₅₋₃₅-Induced Increased Expression of Pro-Inflammatory Cytokine TNF-α

TNF-α mRNA expression was significantly increased by Aβ₂₅₋₃₅ administration as early as 4 h of incubation ($p < 0.05$), but the increase in protein expression could not be found until 12 h of incubation with Aβ₂₅₋₃₅ ($p < 0.01$). Pretreatment with 4-2A alone did not significantly affect TNF-α expression either in mRNA or in protein levels, but it could partially but significantly decrease the effect of Aβ₂₅₋₃₅ (mRNA expression: $p < 0.05$ and protein expression $p < 0.01$, Figure 7).

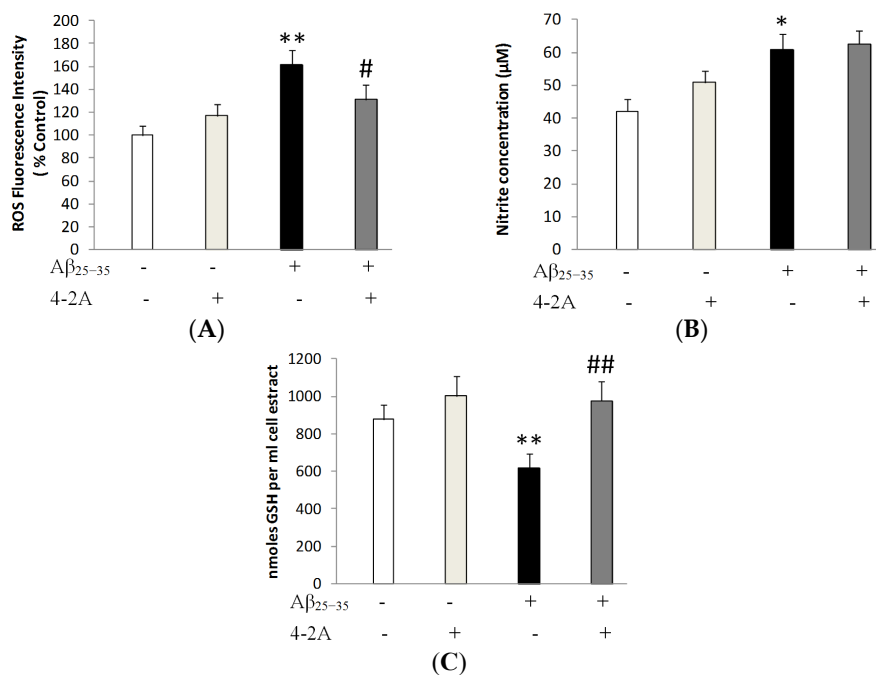


Figure 6. The effect of 4-2A on the changes of oxidative and anti-oxidative response induced by Aβ₂₅₋₃₅. (A) ROS production in fully differentiated SH-SY5Y cells treated with Aβ₂₅₋₃₅ 20 μM and/or 4-2A 10 μM for 24 h. Data represent mean ± SEM percentage of control. (B) NO production and (C) GSH content in fully differentiated SH-SY5Y cells treated with Aβ₂₅₋₃₅ 20 μM and/or 4-2A 10 μM for 24 h. Data represent mean ± SEM of concentration (μM per mL). The statistics were based on data from six separate experiments, $n = 6$ in each experiment. * $p < 0.05$, ** $p < 0.01$ vs. control group; # $p < 0.05$, ## $p < 0.01$ vs. Aβ₂₅₋₃₅ group.

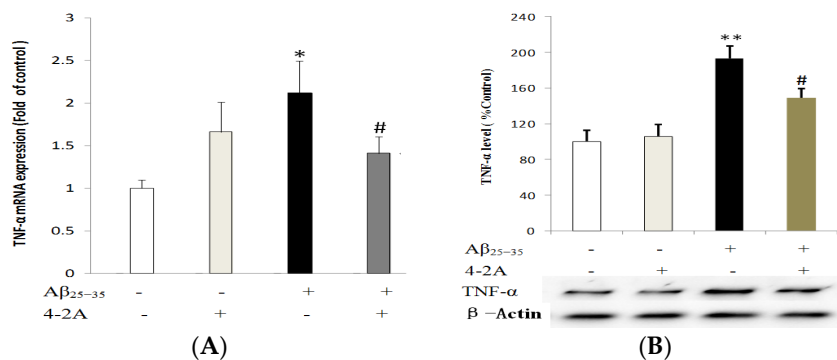


Figure 7. The expression of pro-inflammatory cytokine tumor necrosis factor-α (TNF-α). mRNA expression level (A); and protein expression level (B) of TNF-α, normalized to the corresponding level expression of housekeeping gene β-Actin, in differentiated SH-SY5Y cells treated with Aβ₂₅₋₃₅ (20 μM) and/or 4-2A (10 μg/mL) for indicated times. The data of both mRNA and protein expression from six independent experiments ($n = 1$ in each experiment) were analyzed and expressed as mean ± SEM. * $p < 0.05$, ** $p < 0.01$ vs. control group; # $p < 0.05$ vs. Aβ₂₅₋₃₅ group.

2.5. Effect of 4-2A on the Expression of Neurotrophins: NGF and BDNF and Their TrkA and TrkB Receptors

Similar to TNF-α gene, the obvious change of NGF gene expression appeared at 4 h of Aβ₂₅₋₃₅ treatment. Compared to control group, NGF mRNA expression in Aβ₂₅₋₃₅-insulted cells was significantly down-regulated ($p < 0.01$, Figure 8A). Meanwhile, BDNF gene mRNA expression in Aβ₂₅₋₃₅-insulted cells was also down-regulated at both 4 and 8 h ($p < 0.01$, Figure 8B). Compared

to the control, a significantly decreased protein expression of NGF was found until 12 h incubation ($p < 0.01$, Figure 8C), whereas BDNF protein was significantly increased in $A\beta_{25-35}$ -insulted cells ($p < 0.01$, Figure 8D). However, in cells treated with 4-2A only, either NGF or BDNF gene was not affected at both mRNA and protein level compared to the control ($p > 0.05$). 4-2A pre-treatment could partially but significantly attenuate the $A\beta_{25-35}$ -induced change in NGF mRNA ($p < 0.05$) and protein ($p < 0.01$) expression (Figure 8A,C) and BDNF mRNA expression (both $p < 0.01$, Figure 8D), but not in BDNF protein expression ($p > 0.05$, Figure 8D).

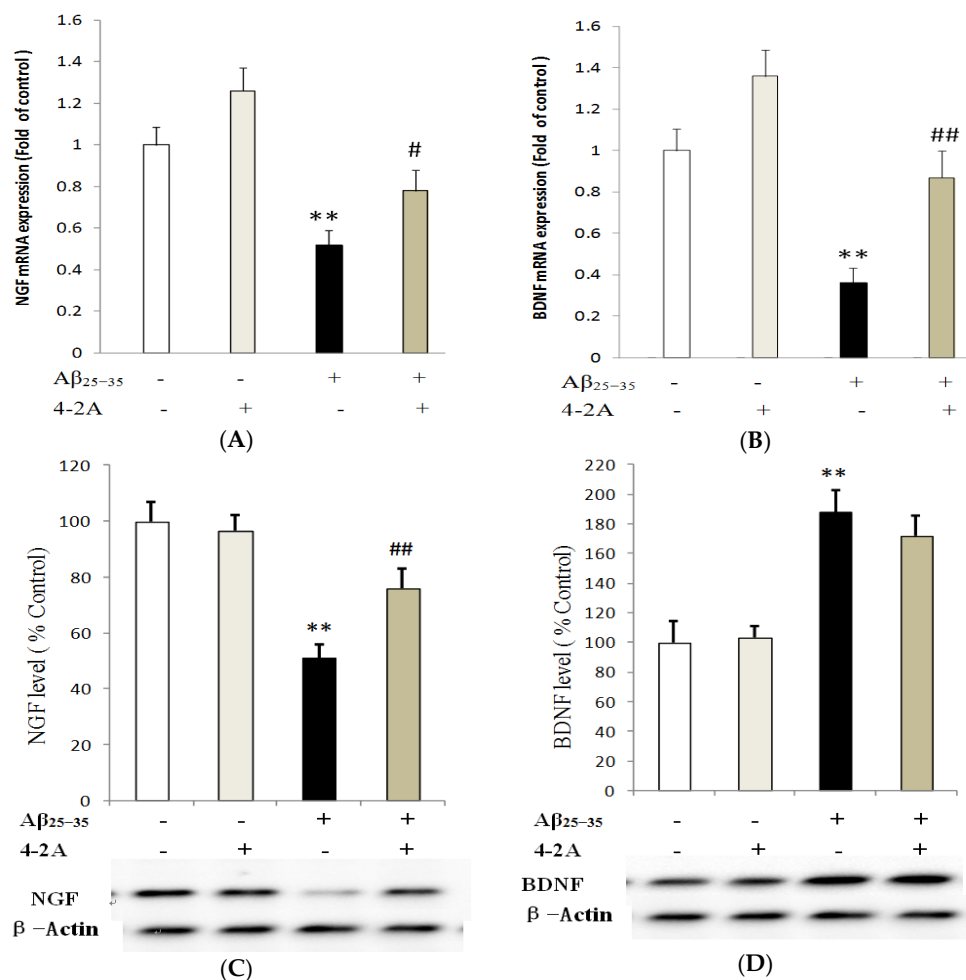


Figure 8. The effect of 4-2A on the expression of neurotrophin genes: NGF and BDNF. NGF mRNA expression (A); and protein expression (C); and BDNF mRNA expression (B); and protein expression (D), normalized to the expression of housekeeping gene β -Actin, in differentiated SH-SY5Y cells treated with $A\beta_{25-35}$ (20 μ M) and/or 4-2A (10 μ g/mL) for 4, 8, 12, 24 h. The data of both mRNA and protein expression from six independent experiments ($n = 1$ in each experiment) were analyzed and expressed as mean \pm SEM. ** $p < 0.01$ vs. control group; # $p < 0.05$, ## $p < 0.01$ vs. $A\beta_{25-35}$ group.

Unlike previously discussed genes, TrkA and TrkB were only affected at 24 h following $A\beta_{25-35}$ administration. $A\beta_{25-35}$ significantly decreased TrkA protein expression ($p < 0.01$). Pretreatment with 4-2A only had no effect on TrkA protein expression, but it could significantly attenuate the effect of $A\beta_{25-35}$ on the receptor ($p < 0.01$, Figure 9A). In contrast to TrkA changes, TrkB protein in the cells treated with 4-2A only was significantly increased ($p < 0.01$) compared to the control. In the cells administrated with $A\beta_{25-35}$ alone, a less but significantly increased protein of TrkB was also found ($p < 0.05$). 4-2A pretreatment did not reverse $A\beta_{25-35}$ -induced change, but further increased in TrkB expression ($p < 0.05$, Figure 9B).

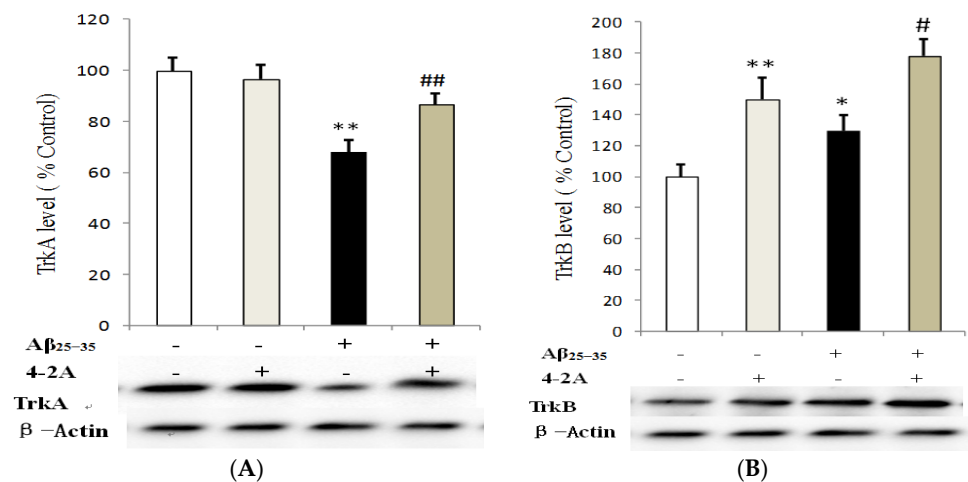


Figure 9. The effect of 4-2A on the expression of neurotrophin receptors: TrkA and TrkB. TrkA (A); and TrkB (B) protein expression, normalized to the protein expression of housekeeping gene β -Actin, in differentiated SH-SY5Y cells treated with $A\beta_{25-35}$ (20 μ M) and/or 4-2A (10 μ g/mL) for 24 h. The data of protein expression from six independent experiments ($n = 1$ in each experiment) were analyzed and expressed as mean \pm SEM. * $p < 0.05$, ** $p < 0.01$ vs. control group; # $p < 0.05$, ## $p < 0.01$ vs. $A\beta_{25-35}$ group.

2.6. Treatment with 4-2A Regulated the Expression of Apoptosis Related Genes: Bax, Bcl-2 and Caspase-3

The genes Bax, Bcl-2 and Caspase-3 protein expression were tested at different incubation times with $A\beta_{25-35}$ (4, 8, 12 and 24 h). The expression of Bcl-2 was strongly decreased by $A\beta_{25-35}$ at 24 h of incubation with $A\beta_{25-35}$, which was significantly increased ($p < 0.01$) by 4-2A. 4-2A by itself had no effect on Bcl-2. With regard to Bax, no obvious change was found after 4–24 h incubation. The Bax: Bcl-2 ratio was significantly increased in cells administrated with $A\beta_{25-35}$ alone ($p < 0.01$). Pretreatment with 4-2A significantly reversed the ratio of Bax: Bcl-2 to the control level ($p < 0.01$, Figure 10A). For Caspase-3, $A\beta_{25-35}$ significantly increased its protein expression ($p < 0.01$), whereas pretreatment with 4-2A only did not affect the expression, but it could partially attenuate the effect of $A\beta_{25-35}$ ($p < 0.05$, Figure 10B).

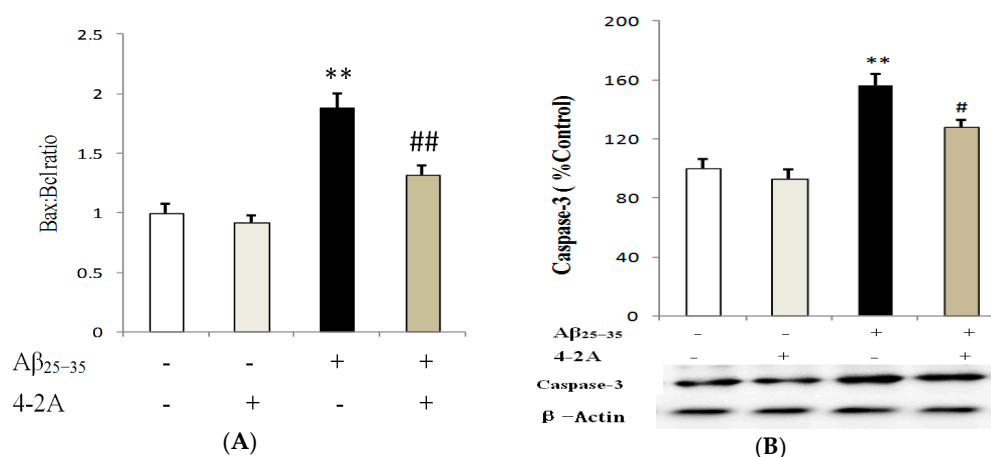


Figure 10. 4-2A regulated the expression of apoptosis related genes: Bcl-2, Bax and Caspase-3. Bax:Bcl-2 ratio (A); and Caspase-3 (B) protein expression (normalized to the protein expression of housekeeping gene β -Actin) in differentiated SH-SY5Y cells treated with $A\beta_{25-35}$ 20 μ M and/or 4-2A 10 μ g/mL for 24 h. The data of both mRNA and protein expression from six independent experiments ($n = 1$ in each experiment) were analyzed and expressed as mean \pm SEM. ** $p < 0.01$ vs. control group; # $p < 0.05$, ## $p < 0.01$ vs. $A\beta_{25-35}$ group.

3. Discussion

A β_{25-35} , an active fragment corresponding to amino acids 25–35 in full-length A β , possesses the same β -sheet structure and retains full toxicity of full-length A β_{1-42} [29]. Many experiments have demonstrated that A β_{25-35} can induce neurotoxicity and AD-like pathology, such as activating glial cells, increasing cholinesterase expression [30] and oxidative stress [31], as well as impairing spatial learning and memory [32,33]. Our previous study also showed that A β_{25-35} could result in neuroinflammatory response and dysfunction of neurotrophin system [34]. As such, A β_{25-35} has been popularly utilized to induce in vitro or in vivo AD models [32,33,35,36]. The present study demonstrates that 4-2A protects the SH-SY5Y cells from A β_{25-35} -induced reduction in cell viability by suppressing oxygen stress and inflammation, regulating neurotrophin levels, hence attenuating neuron apoptosis.

Even though the exact pathophysiology of AD is unclear, oxidative stress has been found to play a fatal role in the pathogenic process of AD. Previous studies demonstrated that toxicity of A β_{25-35} in models of neurodegenerative diseases in vitro and in vivo was associated with the enhancement of ROS and NO liberation and oxidative damage [37–41], which up-regulated redox-sensitive transcription factors such as NF- κ B, an important factor responsible for oxidative and inflammatory reactions in AD [42]. In agreement with these studies, A β_{25-35} increased the ROS and NO production from SH-SY5Y cells in the present study. ROS and NO are oxidants in the Alzheimer's brain. However, NO is also a neurotransmitter, which may protect synapses by increasing neuronal excitability [43,44]. Thus, whether the A β -induced increase in NO acts as a compensatory and neuroprotective or neurotoxic role is unclear. The administration of 4-2A into A β_{25-35} -treated cells partially but significantly decreased ROS production, which means 4-2A may partially protect neurons against free radicals or may improve mitochondrial dysfunction which is the major source of ROS. Furthermore, the decrease in GSH content caused by A β_{25-35} was significantly attenuated by 4-2A treatment. These findings indicated that 4-2A could restore the imbalance between oxidative stress factors and antioxidant systems. However, 4-2A could not affect the A β_{25-35} -induced NO change, which may be related to a hypothesis that 4-2A may contribute to the self-protective ability of A β -insulted cells if this increase in NO is neuroprotective.

Inflammation is another important contributor to neurodegenerative diseases. Experimental and clinical findings provide evidence for the hypothesis that the neuronal degeneration in AD is not simply due to the A β deposition, but to neuroinflammation [45,46]. Consistent with the above studies, an increased expression of TNF- α gene was found in the present AD cellular model. Increased TNF- α can activate a pro-apoptotic factor JNK pathway that is involved in cell differentiation and proliferation [47] and trigger cellular death signaling [27]. In the present study, 4-2A showed anti-inflammatory property since it partially down-regulated the expression of TNF- α either in the mRNA or in protein level.

In our previous study, we showed that neuroinflammation could reduce the levels of neurotrophic factors, such as NGF [48] and BDNF [49]. In the present study, A β_{25-35} differently regulated the expression of the two neurotrophic factor genes. The decreased expression of NGF and its receptor TrkA seems to be reasonable for the low neuronal viability induced by A β . However, a significant increase in the expression of BDNF and its receptor TrkB protein in SH-SY5Y cells exposed to A β_{25-35} was unexpected, which was unparalleled by the decreased mRNA level in BDNF. The present data are partially in agreement with a previous in vitro study showing that the exposure of SH-SY5Y cells to A β_{25-35} induced a significant increase of BDNF [50]. We speculate that the increase of BDNF levels might act as a compensatory response against amyloid toxicity, while A β_{25-35} may trigger distinct effects on BDNF expression in different systems, conditions and incubation time.

Over-production of pro-inflammatory cytokines, oxidative stress and neurotrophin dysfunction may reduce neurogenesis and induce apoptosis [51,52], which result in neuronal death and memory loss in AD [53–56]. In the present study, A β_{25-35} treatment increased the pro-apoptotic Bax/anti-apoptotic Bcl-2 ratio and Caspase-3 expression, which were attenuated by pretreatment of 4-2A, suggesting 4-2A can regulate the imbalance between pro- and anti-apoptotic gene expression. The mechanism by which 4-2A attenuated A β -induced neuron damage may be through its unique components.

The acetone extract 4-2A from the shrimp by-products consists of lipids containing large amount of unsaturated fatty acids, especially monounsaturated fatty acid (MUFAs, 67.19%), including *n*-9 MUFAs and *n*-7 MUFAs. Oleic acid (18:1*n*-9) and palmitoleic acid (16:1*n*-7) are the most common MUFAs, which represent *n*-9 and *n*-7 MUFAs, respectively. The total fatty acids analysis profiles that 18:1*n*-9 (oleic acid, 20.65%) is the most abundant fatty acid in 4-2A. As the major *n*-9 MUFAs, oleic acid is high in olive oil which is the main characteristic of the Mediterranean Style Diet (MSD). Recent data from large epidemiological studies suggest a relationship between MSD adherence and significant reduction in incidence of Parkinson's disease and AD and mild cognitive decline or risk of dementia [57]. Moreover, the protective effect of oleate against palmitate-induced mitochondrial dysfunction, insulin resistance and inflammatory signaling has been evaluated in several cell models [17,58]. Interestingly, in neuronal cells, Kwon et al. demonstrated that oleate preconditioning was superior to DHA or linoleate (18:2*n*-6) in the protection from the above palmitate-induced insults [58]. These effects may be associated with the neuroprotective ability of 4-2A to exert anti-inflammatory effects and restore the imbalance between oxidative stress factors and antioxidant systems. In addition, oleic acid may behave as a neurotrophic factor for neurons via up-regulation of molecular markers of axonal and dendritic growth, such as GAP-43 and MAP-2 [20]. This may be an important factor related to the ability of 4-2A to modulate A β ₂₅₋₃₅-induced abnormality in neurotrophic systems. These results strongly suggest that the ability of 4-2A to prevent SH-SY5Y cells from neurotoxicity induced by A β ₂₅₋₃₅ may be associated with its high content of oleic acid.

In recent years, *n*-7 palmitoleic acid (16:1*n*-7, 14.75%) has drawn increasing attention since its characterization as a bioactive lipid that coordinates metabolic crosstalk between the liver and adipose tissue [59]. Studies in cultured hepatocytes and mouse models of diet-induced obesity suggest that palmitoleic acid has anti-inflammatory and insulin-sensitizing effects [60]. Moreover, both in vitro and in vivo studies have demonstrated that palmitoleic acid can decrease the level of pro-inflammatory mediators and reduce the level of C-reactive protein in mice [21,23]. These anti-inflammatory effects may also contribute to the neuro-protective effect of 4-2A in the present study. However, because of rare reports about the effect of other MUFAs in health, the role of other two *n*-9 MUFAs (20:1*n*-9 and 22:1*n*-9) and three *n*-7 MUFAs (18:1*n*-7, 20:1*n*-7 and 22:1*n*-7) of longer chain length (\geq C18) in 4-2A is unclear.

It is not surprising that 4-2A could protect SH-SY5Y neurons-like cells against A β ₂₅₋₃₅-induced apoptosis and death since 4-2A is rich in polyunsaturated *n*-3 fatty acids, such as EPA and DHA. Our previous studies have confirmed that *n*-3 fatty acids possess broad spectrum of neuroprotective activities in both in vitro and in vivo experiments because of their anti-oxidant and anti-inflammatory properties [61–66]. Additionally, Wu et al. [67] showed that *n*-3 PUFAs significantly attenuated the gene expression of pro-inflammatory cytokines, including IL-1 β , IL-6, and TNF- α , and the protein levels of NF- κ B and iNOS in brain tissues of rats with doxorubicin-induced depressive-like behaviors and neurotoxicity. In another in vivo study, Taepavarapruk and Song [48] revealed that *n*-3 PUFAs improved memory through IL-1-glucocorticoid-ACh release and IL-1-NGF-ACh release pathways. Moreover, there is evidence that dietary supplementation with DHA reduced the intraneuronal accumulation of not only amyloid-beta, but also tau, another important pathology marker for AD, in the 3xTg-AD mouse model via decreasing steady-state levels of presenilin 1 [68,69]. Based on these findings, there is no doubt that the neuroprotective effect of 4-2A was related to the rich *n*-3 PUFAs component. As the concentration of *n*-6 PUFAs are very low (1.85%), their effect in 4-2A can be ignored.

Finally, the saturated fatty acid in 4-2A may have no effect or only serve as an energy component in the cell cultural system because no biological activity was reported.

Taken together, shrimp processing by-product acetone extract 4-2A was prepared and characterized as lipids consisting of large amount of unsaturated fatty acids by NMR, HPLC-CAD and GC analyses. As a multifunctional agent, 4-2A showed potent inhibition against A β ₂₅₋₃₅ cytotoxicity, which confirms our hypothesis that 4-2A may exert neuroprotective effect via anti-oxidant, anti-inflammation and increasing neurotrophins. These effects of 4-2A may result from its various FAs

components targeting various molecular pathways. The limitations of the present study are firstly that the treatment of 4-2A should be studied in the animal model of AD. Secondly, the effect of each FA component and their combination in different ratios should be determined, which can reveal the exact role of each FA and potential synergistic action of their combination in inflammatory, oxidant and neurotrophic functions in the brain. Thirdly, as the main components of neuronal membranes, the effect of FAs in 4-2A on the function of cell membrane and other mechanisms involved should also be investigated.

4. Materials and Methods

4.1. Preparation of the Shrimp Extract 4-2A

Fatty acids from the solid residue of shrimp *Pandalus borealis* processing waste were extracted with hexane (15 mL/g, *v/w* dry weight) at room temperature for 30 min, followed by 10 min of sonication, filtered, and then extracted with acetone under the same conditions. The liquid acetone extracts were combined, concentrated using rotary evaporator at reduced pressure, and then dried under N₂. The resulting extract was named 4-2A.

4.2. Characterization of Shrimp Extract 4-2A

4.2.1. Characterization of 4-2A by NMR

Both ¹H-NMR and ¹³C-NMR spectra of 4-2A (1 mg, dissolved in 700 μL of 99.8% CDCl₃) were recorded at 4 °C on a Bruker AV-III 700 MHz spectrometer (Bruker BioSpin Canada, Milton, ON, Canada), equipped with a 5 mm TCI cryoprobe. The data were processed using the standard TopSpin V 2.1 (Bruker BioSpin Canada, Milton, ON, Canada) software.

4.2.2. Characterization of 4-2A by HPLC

HPLC analysis was carried out on an 1100 series instrument (Agilent Technologies, Santa Clara, CA, USA) with a Thermo Scientific™ Dionex™ Corona™ Charged Aerosol Detector (Burlington, ON, Canada). The method was adopted from dionex.com [70] with modifications. Samples were prepared by diluting 1 mg of analyte in 1 mL of methanol/chloroform (1:1, *v/v*). Ten microliter of each sample solution was injected on a HALO C8 column (2.1 mm × 100 mm, 2.7 μm, Advanced Materials Technology Inc., Wilmington, DE, USA) with a 0.45 mL/min flow rate at 40 °C. A 5 × 2.1 mm C8 cartridge (2.7 μm, Advanced Materials Technology Inc.) was used as a pre-column. Mobile phase A methanol/water/acetic acid (750:250:4) and phase B acetonitrile/methanol/tetrahydrofuran/acetic acid (500:375:125:4) were proceeded from 100% A at the beginning at 0.8 mL/min to 30% A and 70% B at 40 min at 1.0 mL/min, then reached to 20% A and 80% B in 10 min at 1.0 mL/min and finally to 100% B in 10 min at 1.0 mL/min, held for 10 min, and then back to 100% A in 10 min at 0.8 mL/min. The column temperature was at 40 °C.

Free fatty acids (myristic acid, *cis*-palmitoleic acid, *cis*-vaccenic acid, *trans*-vaccenic acid, oleic acid, elaidic acid, pentadecanoic acid, palmitic acid, heptadecanoic acid, *cis*-10-heptadecenoic acid, stearic acid, 9-*cis*,12-*cis*-linoleic acid, *cis,cis,cis*-9,12,15-octadecatrienoic acid, *cis,cis,cis*-6,9,12-octadecatrienoic acid, *cis*-11-eicosenoic acid, arachidonic acid, *cis*-5,8,11,14,17-eicosapentaenoic acid, *cis*-4,7,10,13,16,19-docosahexaenoic acid and tricosanoic acid), monoglycerides (DL- α -palmitin, 1-monopalmitoleoyl-*rac*-glycerol and 1-Oleoyl-*rac*-glycerol), diglycerides (1,2-distearoyl-*rac*-glycerol and 1,3-distearoylglycerol), triglycerides (olive oil), and phospholipids mixer (L- α -lysophosphatidylcholine, L- α -phosphatidylcholine, L- α -phosphatidylethanolamine and L- α -phosphatidylinositol sodium salt) purchased from Sigma-Aldrich Inc. (St. Louis, MO, USA) were applied on the column under the same conditions.

4.2.3. GC Analysis of 4-2A

GC analysis was performed as described by Jiao et al. [25]. Total fatty acids were released from 4-2A by hydrolyzing with 1.5 N NaOH methanol solution under N₂ at 100 °C for 5 min, then

methylated with 14% of BF_3 methanol solution at $100\text{ }^\circ\text{C}$ for 30 min. Distilled water was then added to stop the reaction. The methylated fatty acids were extracted with hexane and subjected on an Agilent Technologies 7890A GC spectrometer (Agilent Technologies, Santa Clara, CA, USA) using an Omegawax 250 fused silica capillary column ($30\text{ m} \times 0.25\text{ mm} \times 0.25\text{ }\mu\text{m}$ film thickness, Sigma-Aldrich, St. Louis, MO, USA). Supelco[®] 37 component fatty acid methylated esters (FAME) mix and PUFA-3 (Supelco, Bellefonte, PA, USA) were used as FAME standards.

4.3. SH-SY5Y Culture and Differentiation

SH-SY5Y cells were obtained from ATCC (CRL-2266, Lot. 61983120) and were maintained in DMEM/F12 medium (Gibco[®], Burlington, ON, Canada) supplemented with 10% fetal bovine serum (FBS, Gibco[®], Burlington, ON, Canada) and 1% penicillin–streptomycin in a humid atmosphere of 5% CO_2 at $37\text{ }^\circ\text{C}$. SH-SY5Y cells were differentiated into fully human neuron-like cells with treatment all-*trans*-retinoic acid (RA, Sigma Aldrich, Oakville, ON, Canada), at a final concentration of $10\text{ }\mu\text{M}$ in DMEM/F12 with 3% FBS (media changed every 2 days), for 7–8 days.

4.4. Experimental Design

Once the SH-SY5Y cells were differentiated into classic neuron-like cells with long axons compared to undifferentiated cells, they were used in the experiments. $\text{A}\beta_{25-35}$ (synthetic, $\geq 97\%$ HPLC, Sigma Aldrich, Oakville, ON, Canada, A4559) was dissolved in sterile double-distilled water at a concentration of 1 mmol/L stock solution, was aged at $37\text{ }^\circ\text{C}$ for 4 day, and then stored at $-20\text{ }^\circ\text{C}$ before use (This aging procedure was proved to produce birefringent fibril-like structures, globular amorphous aggregates and induce cognitive impairment in rats [34,71]). The 4-2A was dissolved in ethanol at a stock concentration of 100 mg/mL , and then added to DMEM/F12 (final ethanol concentration 0.1%). The effects of $\text{A}\beta_{25-35}$ at 5, 10, 15, 20 and $25\text{ }\mu\text{M}$ at 12, 24 and 48 h and the effects of 4-2A at 1, 5, 10, 20 and $40\text{ }\mu\text{g/mL}$ on $\text{A}\beta_{25-35}$ -induced SH-SY5Y cell injury were then determined separately. The optimal dose and culture duration of $\text{A}\beta_{25-35}$ ($20\text{ }\mu\text{M}$, 24 h) and 4-2A ($10\text{ }\mu\text{g/mL}$, pretreated for 12 h before addition of $20\text{ }\mu\text{M}$ $\text{A}\beta_{25-35}$) were selected based on when the significant decrease in cell viability or attenuation of this effect appeared respectively. In the present study, four groups of SH-SY5Y cells were used: (i) control (cells in culture media which contained 0.1% *v/v* ethanol); (ii) 4-2A (cells in culture media with $10\text{ }\mu\text{g/mL}$ 4-2A); (iii) $\text{A}\beta_{25-35}$ (cells in culture media with $20\text{ }\mu\text{M}$ $\text{A}\beta_{25-35}$); and (iv) 4-2A and $\text{A}\beta_{25-35}$ (cells pretreated with $10\text{ }\mu\text{g/mL}$ 4-2A for 12 h before addition of $20\text{ }\mu\text{M}$ $\text{A}\beta_{25-35}$). After the addition of $\text{A}\beta_{25-35}$, the SH-SY5Y cells were incubated for 24 h, after which cell viability, oxidative stress, inflammatory cytokine TNF- α , neurotrophins and apoptosis were measured.

4.5. Measurement of Cell Viability by MTT Assay

Cell viability was measured using MTT assay which measures the cell proliferation rate and the reduction in cell viability. Cells were seeded in 96-well plates and $90\text{ }\mu\text{L}$ of cell suspension added to each well. Following experimental treatment, $10\text{ }\mu\text{L}$ MTT (ATCC) was added to each well and the plate was incubated for additional 4 h at $37\text{ }^\circ\text{C}$. The optical density was measured at 570 nm using a microplate reader (BioTek, Winooski, VT, USA). The absorbance of the control group was considered as 100% of the cell viability.

4.6. Cytotoxicity Assay by LDH Assay

As MTT assay was sensitive to cell numbers which was affected by both cell proliferation and cell viability, it was essential to use another assay to confirm the result. The CytoTox-96 assay kit (Promega, Madison, WI, USA) was employed to evaluate the total release of cytoplasmic lactate dehydrogenase (LDH) into the medium, which is a consequence of cellular integrity damage. The assay is based upon a coupled enzymatic conversion from 2-*p*-(iodophenyl)-3-(*p*-nitrophenyl)-5-phenyltetrazolium chloride (INT, a tetrazolium salt) into a formazan product, and the enzymatic reaction is catalyzed by LDH released from cells and diaphorase in the assay substrate mixture. Absorbance was read at 490 nm by

the microplate reader. The mean absorbance of each group was normalized to the percentage of the control value.

4.7. Measurement of Oxidative Stress and Antioxidant Response

The intracellular level of ROS was measured with a fluorometric intracellular ROS kit (Sigma Aldrich) according to manufacturer's instructions. The fluorescence intensity was detected at $\lambda_{ex} = 650/\lambda_{em} = 675$ nm using a fluorescence microplate reader (Reader Synergy HT, BioTek). The intracellular level of NO production was determined by the Griess Reagent System (Promega) according to manufacturer's instructions. The absorbance was measured at 540 nm using a microplate reader.

The level of GSH was determined with a glutathione assay kit (Sigma Aldrich) according to manufacturer's instructions. The fluorescence intensity was measured by a fluorimeter plate reader set at an excitation wavelength of 390 nm and emission wavelength of 478 nm.

4.8. Determination of Gene Expression with Quantitative PCR

SH-SY5Y cells treated as described above were harvested. The total RNA was extracted as recommended by the manufacturer (RNeasy[®] Lipid Tissue Handbook, Qiagen, Germantown, MD, USA). Complementary DNA (cDNA) was synthesized from 2 μ g RNA using the GoScript[™] Reverse Transcriptase (Promega, Madison, WI, USA). Primer sequences (Table 2) were obtained from Invitrogen Corporation. PCR reactions were prepared using Quantitect SYBR Green master mix (Qiagen, Germantown, MD, USA) and carried out using a Real-Time PCR Detection Systems (Bio-Rad, Hercules, CA, USA) CFX96[™] Real-Time System. The real-time PCR was optimized to run with conditions of the initial incubation at 95 °C for 5 min, denaturation at 94 °C for 15 s, annealing at 59 °C for 30 s, and extension at 72 °C for 30 s with a single fluorescence measurement and up to 38 cycles. Expression levels of target mRNAs were normalized to beta actin (relative quantification) with the $\Delta\Delta$ CT correction.

Table 2. Primer names and sequences.

Primer Names	Sequences
hActin F	GATGAGATTGGCATGGCTTT
hActin R	CACCTTCACCGTCCAGTTT
hBAX F	GGGGACGAACTGGACAGTAA
hBAX R	CAGTTGAAGTTGCCGTCAGA
hBCL 2 F	TCTAGGGGAGGTGGTAGGCT
hBCL 2 R	CTGAGCAAGTCAGAGACCCC
hCaspase 3 F	GACTCTAGACGGCATCCAGC
hCaspase 3 R	TGACAGCCAGTGAGACTTGG
hNGF F	ACCTTTCTCAGTAGCGGCAA
hNGF R	TGTGTCACCTTGT CAGGGAA
hTNF- α F	AGGTTTGGCCTCACAAGGAC
hTNF- α R	GCGGTAGGGACAGTTCACAG
hBDNF F	GGAGACACATCCAGCAAT
hBDNF R	ACAAGAACGAACACAACAG
hTrkB F	CTATGCTGTGGTGGTGATT
hTrkB R	CCGAAGAAGATGGAGTGTTA
hTrkA F	TACAGCACCGACTATTACC
hTrkA R	ATGATGGCGTAGACCTCT

4.9. Analysis of Protein Expression by Western Blotting

SH-SY5Y cells treated as described above were collected and centrifuged at $10,000\times g$ for 10 min. The cell pellet was lysed with a RIPA buffer (RIPA, Thermo Fisher Scientific, Hudson, NH, USA) aided by sonication, and then spun down at $10,000\times g$ for 10 min at $4\text{ }^{\circ}\text{C}$. The supernatant was collected and aliquots containing 20–40 μg of protein were loaded after boiling and separated on 10% SDS PAGE gels at 100 V for 60 min in electrophoresis buffer. After running the gels, the proteins were transferred to Polyvinylidene difluoride (PVDF) membranes (Millipore, Bellerica, MA, USA). The membranes were blocked with 5% non-fat milk in Tris buffer saline for 1 h at $20\text{ }^{\circ}\text{C}$. Following blocking, blots were washed with TBST for 5 min and incubated with primary antibodies, including the rabbit origin polyclonal antibodies for Actin (Abcam, Cambridge, MA, USA; ab8227, 42 kDa, 1:4000), NGF (Abcam, ab52918, 27 kDa, 1:500), BDNF (Abcam, ab6201, 28kDa, matured form, 1:200), TrkA (Abcam, ab59272, 85 kDa, 1:800), TrkB (Thermo Fisher Science, Hudson, NH, USA; MA5-14903, 90-140 kDa, 1:1000), TNF- α (Abcam, ab9739, 17 kDa, 1:2500), Bcl-2 (Abcam, ab136285, 26 kDa, 1:5000), Bax (Abcam, ab32503, 21 kDa, 1:2000) and Caspase-3 (Abcam, ab44976, 32 kDa, activated forms, 1:500), overnight at $4\text{ }^{\circ}\text{C}$, followed by the secondary antibody, peroxidase (HRP)-conjugated anti-rabbit IgG (Abcam, ab6721, 1:5000), for 1 h at $20\text{ }^{\circ}\text{C}$. The blots were washed in TBS three times. Immunoreactive bands were detected by Clarity™ Western ECL Substrate Kit (Bio-Rad, Hercules, CA, USA) on a ChemiDoc™ MP System with Image Lab™ Software (Bio-Rad, Hercules, CA, USA). All target proteins were quantified by normalizing them to β -Actin re-probed on the same membrane and then calculated as a percentage of the control group.

4.10. Statistics

Results were expressed as mean \pm SEM. Statistical evaluation was performed with IBM SPSS Statistics 22. For the dose–response test of 4-2A / A β_{25-35} , results were analyzed by one-way ANOVA, followed by Dunnett post-hoc test in case of significant main effects ($p < 0.05$). The possible interaction between A β_{25-35} and 4-2A was measured by two-way ANOVA with Tukey’s post-hoc tests. A value of $p < 0.05$ was considered statistically significant.

Acknowledgments: This study was supported by grants to Cai Song by Atlantic Innovation Fund of Canada, National Natural Science Foundation of China (No. 81171118 and No. 81471223), Project of Enhancing School with Innovation of Guangdong Ocean University (GDOU2013050110) and Project of Science and Technology of Zhanjiang of China. Guanglin Jiao and Junzeng Zhang were supported by Natural Health Product (NHP) Program of National Research Council of Canada. We would like to thank Island Fishermen Cooperative Association (IFCA) processing plant for providing the shrimp byproducts.

Author Contributions: C.S., Y.Z., J.Z., J.G., and G.J. conceived and designed the experiments; Y.Z., G.J. and S.G. performed the experiments; Y.Z. and G.J. analyzed the data; R.E.B., J.G., P.Z. Y.Z. and H.L. contributed to materials, analytical methods, data interpretation and discussion; C.P., R.S., and S.L. contributed to sample analysis and data verification; Y.Z., and C.S. wrote the paper with all others contributing in editing and revision.

Conflicts of Interest: The authors declare no conflict of interest.

References

1. Selkoe, D.J. Alzheimer’s disease. *Cold Spring Harbor Perspect. Biol.* **2011**, *3*. [[CrossRef](#)] [[PubMed](#)]
2. Kumar, S.; Okello, E.J.; Harris, J.R. Experimental inhibition of fibrillogenesis and neurotoxicity by amyloid-beta (Abeta) and other disease-related peptides/proteins by plant extracts and herbal compounds. *Sub-Cell. Biochem.* **2012**, *65*, 295–326.
3. Selkoe, D.J.; Hardy, J. The amyloid hypothesis of Alzheimer’s disease at 25 years. *EMBO Mol. Med.* **2016**, *8*, 595–608. [[CrossRef](#)] [[PubMed](#)]
4. Kim, H.G.; Moon, M.; Choi, J.G.; Park, G.; Kim, A.J.; Hur, J.; Lee, K.T.; Oh, M.S. Donepezil inhibits the amyloid-beta oligomer-induced microglial activation in vitro and in vivo. *Neurotoxicology* **2014**, *40*, 23–32. [[CrossRef](#)] [[PubMed](#)]

5. Tabner, B.J.; Turnbull, S.; King, J.E.; Benson, F.E.; El-Agnaf, O.M.; Allsop, D. A spectroscopic study of some of the peptidyl radicals formed following hydroxyl radical attack on beta-amyloid and alpha-synuclein. *Free Radic. Res.* **2006**, *40*, 731–739. [[CrossRef](#)] [[PubMed](#)]
6. Choi, D.J.; Cho, S.; Seo, J.Y.; Lee, H.B.; Park, Y.I. Neuroprotective effects of the *Phellinus linteus* ethyl acetate extract against H₂O₂-induced apoptotic cell death of SK-N-MC cells. *Nutr. Res.* **2016**, *36*, 31–43. [[CrossRef](#)] [[PubMed](#)]
7. Sondag, C.M.; Dhawan, G.; Combs, C.K. Beta amyloid oligomers and fibrils stimulate differential activation of primary microglia. *J. Neuroinflamm.* **2009**, *6*, 1. [[CrossRef](#)] [[PubMed](#)]
8. Lee, M.; McGeer, E.; McGeer, P.L. Activated human microglia stimulate neuroblastoma cells to upregulate production of beta amyloid protein and tau: Implications for Alzheimer's disease pathogenesis. *Neurobiol. Aging* **2015**, *36*, 42–52. [[CrossRef](#)] [[PubMed](#)]
9. Allen, S.J.; Watson, J.J.; Dawbarn, D. The neurotrophins and their role in Alzheimer's disease. *Curr. Neuropharmacol.* **2011**, *9*, 559–573. [[CrossRef](#)] [[PubMed](#)]
10. Ciaramella, A.; Salani, F.; Bizzoni, F.; Orfei, M.D.; Langella, R.; Angelucci, F.; Spalletta, G.; Taddei, A.R.; Caltagirone, C.; Bossu, P. The stimulation of dendritic cells by amyloid beta 1-42 reduces BDNF production in Alzheimer's disease patients. *Brain Behav. Immun.* **2013**, *32*, 29–32. [[CrossRef](#)] [[PubMed](#)]
11. Poon, W.W.; Carlos, A.J.; Aguilar, B.L.; Berchtold, N.C.; Kawano, C.K.; Zograbyan, V.; Yaoprucke, T.; Shelanski, M.; Cotman, C.W. beta-Amyloid (A β) oligomers impair brain-derived neurotrophic factor retrograde trafficking by down-regulating ubiquitin C-terminal hydrolase, UCH-L1. *J. Biol. Chem.* **2013**, *288*, 16937–16948. [[CrossRef](#)] [[PubMed](#)]
12. Kumar, A.; Singh, A.; Ekavali. A review on Alzheimer's disease pathophysiology and its management: An update. *Pharmacol. Rep.* **2015**, *67*, 195–203. [[CrossRef](#)] [[PubMed](#)]
13. Luchtman, D.W.; Meng, Q.; Song, C. Ethyl-eicosapentaenoate (E-EPA) attenuates motor impairments and inflammation in the MPTP-probenecid mouse model of Parkinson's disease. *Behav. Brain Res.* **2012**, *226*, 386–396. [[CrossRef](#)] [[PubMed](#)]
14. Song, C.; Manku, M.S.; Horrobin, D.F. Long-chain polyunsaturated fatty acids modulate interleukin-1 β -induced changes in behavior, monoaminergic neurotransmitters, and brain inflammation in rats. *J. Nutr.* **2008**, *138*, 954–963. [[PubMed](#)]
15. Song, C. Essential fatty acids as potential anti-inflammatory agents in the treatment of affective disorders. *Mod. Trends Pharmacopsychiatry* **2013**, *28*, 75–89.
16. Song, C.; Li, X.; Leonard, B.E.; Horrobin, D.F. Effects of dietary *n*-3 or *n*-6 fatty acids on interleukin-1 β -induced anxiety, stress, and inflammatory responses in rats. *J. Lipid Res.* **2003**, *44*, 1984–1991. [[CrossRef](#)] [[PubMed](#)]
17. Peng, G.; Li, L.; Liu, Y.; Pu, J.; Zhang, S.; Yu, J.; Zhao, J.; Liu, P. Oleate blocks palmitate-induced abnormal lipid distribution, endoplasmic reticulum expansion and stress, and insulin resistance in skeletal muscle. *Endocrinology* **2011**, *152*, 2206–2218. [[CrossRef](#)] [[PubMed](#)]
18. Coll, T.; Eyre, E.; Rodriguez-Calvo, R.; Palomer, X.; Sanchez, R.M.; Merlos, M.; Laguna, J.C.; Vazquez-Carrera, M. Oleate reverses palmitate-induced insulin resistance and inflammation in skeletal muscle cells. *J. Biol. Chem.* **2008**, *283*, 11107–11116. [[CrossRef](#)] [[PubMed](#)]
19. Yuzefovych, L.; Wilson, G.; Rachek, L. Different effects of oleate vs. palmitate on mitochondrial function, apoptosis, and insulin signaling in L6 skeletal muscle cells: Role of oxidative stress. *Am. J. Physiol. Endocrinol. Metab.* **2010**, *299*, E1096–E1105. [[CrossRef](#)] [[PubMed](#)]
20. Bento-Abreu, A.; Tabernero, A.; Medina, J.M. Peroxisome proliferator-activated receptor- α is required for the neurotrophic effect of oleic acid in neurons. *J. Neurochem.* **2007**, *103*, 871–881. [[CrossRef](#)] [[PubMed](#)]
21. Frigolet, M.E.; Gutierrez-Aguilar, R. The Role of the Novel Lipokine Palmitoleic Acid in Health and Disease. *Adv. Nutr.* **2017**, *8*, 173S–181S. [[CrossRef](#)] [[PubMed](#)]
22. Gong, J.; Campos, H.; McGarvey, S.; Wu, Z.; Goldberg, R.; Baylin, A. Adipose tissue palmitoleic acid and obesity in humans: Does it behave as a lipokine? *Am. J. Clin. Nutr.* **2011**, *93*, 186–191. [[CrossRef](#)] [[PubMed](#)]
23. Ouchi, N.; Parker, J.L.; Lugus, J.J.; Walsh, K. Adipokines in inflammation and metabolic disease. *Nat. Rev. Immunol.* **2011**, *11*, 85–97. [[CrossRef](#)] [[PubMed](#)]
24. Tchoukanova, N.; Benoit, G. Method for extracting organic solids and oil from marine organisms enriched with astaxanthin. U.S. Patent App. 14/776,481, 2014.

25. Jiao, G.; Hui, J.; Burton, I.; Thibault, M.-H.; Pelletier, C.; Boudreau, J.; Tchoukanova, N.; Subramanian, B.; Djauoued, Y.; Ewart, S.; et al. Characterization of Shrimp Oil from *Pandalus borealis* by High Performance Liquid Chromatography and High Resolution Mass Spectrometry. *Mar. Drugs* **2015**, *13*, 3849–3876. [[CrossRef](#)] [[PubMed](#)]
26. Morioka, N.; Zhang, F.F.; Nakamura, Y.; Kitamura, T.; Hisaoka-Nakashima, K.; Nakata, Y. Tumor necrosis factor-mediated downregulation of spinal astrocytic connexin43 leads to increased glutamatergic neurotransmission and neuropathic pain in mice. *Brain Behav. Immunity* **2015**, *49*, 293–310. [[CrossRef](#)] [[PubMed](#)]
27. Tezel, G. TNF-alpha signaling in glaucomatous neurodegeneration. *Prog. Brain Res.* **2008**, *173*, 409–421. [[PubMed](#)]
28. Gunstone, F.; Knothe, G. NMR Spectroscopy of Fatty Acids and Their Derivatives. AOCs Lipid Library. Available online: <http://lipidlibrary.aocs.org/Analysis/content.cfm?ItemNumber=40256> (accessed on 21 March 2017).
29. Millucci, L.; Ghezzi, L.; Bernardini, G.; Santucci, A. Conformations and biological activities of amyloid beta peptide 25-35. *Curr. Protein Pept. Sci.* **2010**, *11*, 54–67. [[CrossRef](#)] [[PubMed](#)]
30. Sohanaki, H.; Baluchnejadmojarad, T.; Nikbakht, F.; Roghani, M. Pelargonidin improves memory deficit in amyloid beta25-35 rat model of Alzheimer's disease by inhibition of glial activation, cholinesterase, and oxidative stress. *Biomed. Pharmacother.* **2016**, *83*, 85–91. [[CrossRef](#)] [[PubMed](#)]
31. Vedagiri, A.; Thangarajan, S. Mitigating effect of chrysin loaded solid lipid nanoparticles against Amyloid beta25-35 induced oxidative stress in rat hippocampal region: An efficient formulation approach for Alzheimer's disease. *Neuropeptides* **2016**, *58*, 111–125. [[CrossRef](#)] [[PubMed](#)]
32. Mokhtari, Z.; Baluchnejadmojarad, T.; Nikbakht, F.; Mansouri, M.; Roghani, M. Riluzole ameliorates learning and memory deficits in Abeta25-35-induced rat model of Alzheimer's disease and is independent of cholinergic activation. *Biomed. Pharmacother.* **2017**, *87*, 135–144. [[CrossRef](#)] [[PubMed](#)]
33. Fedotova, J.; Soultanov, V.; Nikitina, T.; Roschin, V.; Ordyan, N.; Hritcu, L. Cognitive-enhancing activities of the polyphenol preparation Ropren(R) in gonadectomized beta-amyloid (25-35) rat model of Alzheimer's disease. *Physiol. Behav.* **2016**, *157*, 55–62. [[CrossRef](#)] [[PubMed](#)]
34. Ji, C.; Song, C.; Zuo, P. The mechanism of memory impairment induced by Abeta chronic administration involves imbalance between cytokines and neurotrophins in the rat hippocampus. *Curr. Alzheimer Res.* **2011**, *8*, 410–420. [[CrossRef](#)] [[PubMed](#)]
35. Diaz, A.; Rojas, K.; Espinosa, B.; Chavez, R.; Zenteno, E.; Limon, D.; Guevara, J. Aminoguanidine treatment ameliorates inflammatory responses and memory impairment induced by amyloid-beta 25-35 injection in rats. *Neuropeptides* **2014**, *48*, 153–159. [[CrossRef](#)] [[PubMed](#)]
36. Yu, H.; Yao, L.; Zhou, H.; Qu, S.; Zeng, X.; Zhou, D.; Zhou, Y.; Li, X.; Liu, Z. Neuroprotection against Abeta25-35-induced apoptosis by *Salvia miltiorrhiza* extract in SH-SY5Y cells. *Neurochem. Int.* **2014**, *75*, 89–95. [[CrossRef](#)] [[PubMed](#)]
37. Briyal, S.; Shepard, C.; Gulati, A. Endothelin receptor type B agonist, IRL-1620, prevents beta amyloid (Abeta) induced oxidative stress and cognitive impairment in normal and diabetic rats. *Pharmacol. Biochem. Behav.* **2014**, *120*, 65–72. [[PubMed](#)]
38. Cioanca, O.; Hritcu, L.; Mihasan, M.; Trifan, A.; Hancianu, M. Inhalation of coriander volatile oil increased anxiolytic-antidepressant-like behaviors and decreased oxidative status in beta-amyloid (1-42) rat model of Alzheimer's disease. *Physiol. Behav.* **2014**, *131*, 68–74. [[CrossRef](#)] [[PubMed](#)]
39. Suganthi, N.; Devi, K.P. Protective effect of catechin rich extract of *Rhizophora mucronata* against β -amyloid-induced toxicity in PC12 cells. *J. Appl. Biomed.* **2016**, *14*, 137–146. [[CrossRef](#)]
40. Arimon, M.; Takeda, S.; Post, K.L.; Svirsky, S.; Hyman, B.T.; Berezovska, O. Oxidative stress and lipid peroxidation are upstream of amyloid pathology. *Neurobiol. Dis.* **2015**, *84*, 109–119. [[CrossRef](#)] [[PubMed](#)]
41. Yue, T.; Shanbin, G.; Ling, M.; Yuan, W.; Ying, X.; Ping, Z. Sevoflurane aggregates cognitive dysfunction and hippocampal oxidative stress induced by beta-amyloid in rats. *Life Sci.* **2015**, *143*, 194–201. [[CrossRef](#)] [[PubMed](#)]
42. Padayachee, E.; Ngqwala, N.; Whiteley, C.G. Association of beta-amyloid peptide fragments with neuronal nitric oxide synthase: Implications in the etiology of Alzheimer's disease. *J. Enzyme Inhib. Med. Chem.* **2012**, *27*, 356–364. [[CrossRef](#)] [[PubMed](#)]

43. Gamper, N.; Ooi, L. Redox and nitric oxide-mediated regulation of sensory neuron ion channel function. *Antioxid. Redox Signal.* **2015**, *22*, 486–504. [[CrossRef](#)] [[PubMed](#)]
44. Ooi, L.; Gigout, S.; Pettinger, L.; Gamper, N. Triple cysteine module within M-type K⁺ channels mediates reciprocal channel modulation by nitric oxide and reactive oxygen species. *J. Neurosci.* **2013**, *33*, 6041–6046. [[CrossRef](#)] [[PubMed](#)]
45. Shadfar, S.; Hwang, C.J.; Lim, M.S.; Choi, D.Y.; Hong, J.T. Involvement of inflammation in Alzheimer's disease pathogenesis and therapeutic potential of anti-inflammatory agents. *Arch. Pharm. Res.* **2015**, *38*, 2106–2119. [[CrossRef](#)] [[PubMed](#)]
46. Heppner, F.L.; Ransohoff, R.M.; Becher, B. Immune attack: The role of inflammation in Alzheimer disease. *Nat. Rev. Neurosci.* **2015**, *16*, 358–372. [[CrossRef](#)] [[PubMed](#)]
47. Wang, Y.L.; He, H.; Liu, Z.J.; Cao, Z.G.; Wang, X.Y.; Yang, K.; Fang, Y.; Han, M.; Zhang, C.; Huo, F.Y. Effects of TNF-alpha on Cementoblast Differentiation, Mineralization, and Apoptosis. *J. Dent. Res.* **2015**, *94*, 1225–1232. [[CrossRef](#)] [[PubMed](#)]
48. Taepavaraprak, P.; Song, C. Reductions of acetylcholine release and nerve growth factor expression are correlated with memory impairment induced by interleukin-1beta administrations: Effects of omega-3 fatty acid EPA treatment. *J. Neurochem.* **2010**, *112*, 1054–1064. [[CrossRef](#)] [[PubMed](#)]
49. Song, C.; Zhang, Y.; Dong, Y. Acute and subacute IL-1beta administrations differentially modulate neuroimmune and neurotrophic systems: Possible implications for neuroprotection and neurodegeneration. *J. Neuroinflamm.* **2013**, *10*, 59. [[CrossRef](#)] [[PubMed](#)]
50. Lattanzio, F.; Carboni, L.; Carretta, D.; Candeletti, S.; Romualdi, P. Treatment with the neurotoxic Aβ_{25–35} peptide modulates the expression of neuroprotective factors Pin1, Sirtuin 1, and brain-derived neurotrophic factor in SH-SY5Y human neuroblastoma cells. *Exp. Toxicol. Pathol.* **2016**, *68*, 271–276. [[CrossRef](#)] [[PubMed](#)]
51. Loo, D.T.; Copani, A.; Pike, C.J.; Whittemore, E.R.; Walencewicz, A.J.; Cotman, C.W. Apoptosis is induced by beta-amyloid in cultured central nervous system neurons. *Proc. Natl. Acad. Sci. USA* **1993**, *90*, 7951–7955. [[CrossRef](#)] [[PubMed](#)]
52. McGeer, E.G.; McGeer, P.L. Neuroinflammation in Alzheimer's disease and mild cognitive impairment: A field in its infancy. *J. Alzheimer's Dis. JAD* **2010**, *19*, 355–361. [[PubMed](#)]
53. Asadi, F.; Jamshidi, A.H.; Khodaghali, F.; Yans, A.; Azimi, L.; Faizi, M.; Vali, L.; Abdollahi, M.; Ghahremani, M.H.; Sharifzadeh, M. Reversal effects of crocin on amyloid beta-induced memory deficit: Modification of autophagy or apoptosis markers. *Pharmacol. Biochem. Behav.* **2015**, *139 Pt A*, 47–58. [[CrossRef](#)] [[PubMed](#)]
54. Pieri, M.; Amadoro, G.; Carunchio, I.; Ciotti, M.T.; Quaresima, S.; Florenzano, F.; Calissano, P.; Possenti, R.; Zona, C.; Severini, C. SP protects cerebellar granule cells against beta-amyloid-induced apoptosis by down-regulation and reduced activity of Kv4 potassium channels. *Neuropharmacology* **2010**, *58*, 268–276. [[CrossRef](#)] [[PubMed](#)]
55. Meng, P.; Yoshida, H.; Tanji, K.; Matsumiya, T.; Xing, F.; Hayakari, R.; Wang, L.; Tsuruga, K.; Tanaka, H.; Mimura, J.; et al. Carnosic acid attenuates apoptosis induced by amyloid-beta 1–42 or 1–43 in SH-SY5Y human neuroblastoma cells. *Neurosci. Res.* **2015**, *94*, 1–9. [[CrossRef](#)] [[PubMed](#)]
56. Sharoar, M.G.; Islam, M.I.; Shahnawaz, M.; Shin, S.Y.; Park, I.S. Amyloid beta binds procaspase-9 to inhibit assembly of Apaf-1 apoptosome and intrinsic apoptosis pathway. *Biochim. Biophys. Acta* **2014**, *1843*, 685–693. [[CrossRef](#)] [[PubMed](#)]
57. Feart, C.; Samieri, C.; Alles, B.; Barberger-Gateau, P. Potential benefits of adherence to the Mediterranean diet on cognitive health. *Proc. Nutr. Soc.* **2013**, *72*, 140–152. [[CrossRef](#)] [[PubMed](#)]
58. Kwon, B.; Lee, H.K.; Querfurth, H.W. Oleate prevents palmitate-induced mitochondrial dysfunction, insulin resistance and inflammatory signaling in neuronal cells. *Biochim. Biophys. Acta* **2014**, *1843*, 1402–1413. [[CrossRef](#)] [[PubMed](#)]
59. Cao, H.; Gerhold, K.; Mayers, J.R.; Wiest, M.M.; Watkins, S.M.; Hotamisligil, G.S. Identification of a lipokine, a lipid hormone linking adipose tissue to systemic metabolism. *Cell* **2008**, *134*, 933–944. [[CrossRef](#)] [[PubMed](#)]
60. Guo, X.; Li, H.; Xu, H.; Halim, V.; Zhang, W.; Wang, H.; Ong, K.T.; Woo, S.L.; Walzem, R.L.; Mashek, D.G.; et al. Palmitoleate induces hepatic steatosis but suppresses liver inflammatory response in mice. *PLoS ONE* **2012**, *7*, e39286. [[CrossRef](#)] [[PubMed](#)]
61. Orr, S.K.; Trepanier, M.O.; Bazinet, R.P. n-3 Polyunsaturated fatty acids in animal models with neuroinflammation. *Prostaglandins Leukot. Essent. Fat. Acids* **2013**, *88*, 97–103. [[CrossRef](#)] [[PubMed](#)]

62. Barros, M.; Poppe, S.; Bondan, E. Neuroprotective Properties of the Marine Carotenoid Astaxanthin and Omega-3 Fatty Acids, and Perspectives for the Natural Combination of Both in Krill Oil. *Nutrients* **2014**, *6*, 1293–1317. [[CrossRef](#)] [[PubMed](#)]
63. Uygur, R.; Aktas, C.; Tulubas, F.; Uygur, E.; Kanter, M.; Erboga, M.; Caglar, V.; Topcu, B.; Ozen, O.A. Protective effects of fish omega-3 fatty acids on doxorubicin-induced testicular apoptosis and oxidative damage in rats. *Andrologia* **2014**, *46*, 917–926. [[CrossRef](#)] [[PubMed](#)]
64. Luchtman, D.W.; Meng, Q.; Wang, X.; Shao, D.; Song, C. Omega-3 fatty acid eicosapentaenoic acid attenuates MPP⁺-induced neurodegeneration in fully differentiated human SH-SY5Y and primary mesencephalic cells. *J. Neurochem.* **2013**, *124*, 855–868. [[CrossRef](#)] [[PubMed](#)]
65. Kou, W.; Luchtman, D.; Song, C. Eicosapentaenoic acid (EPA) increases cell viability and expression of neurotrophin receptors in retinoic acid and brain-derived neurotrophic factor differentiated SH-SY5Y cells. *Eur. J. Nutr.* **2008**, *47*, 104–113. [[CrossRef](#)] [[PubMed](#)]
66. Song, C.; Horrobin, D. Omega-3 fatty acid ethyl-eicosapentaenoate, but not soybean oil, attenuates memory impairment induced by central IL-1beta administration. *J. Lipid Res.* **2004**, *45*, 1112–1121. [[CrossRef](#)] [[PubMed](#)]
67. Wu, Y.Q.; Dang, R.L.; Tang, M.M.; Cai, H.L.; Li, H.D.; Liao, D.H.; He, X.; Cao, L.J.; Xue, Y.; Jiang, P. Long Chain Omega-3 Polyunsaturated Fatty Acid Supplementation Alleviates Doxorubicin-Induced Depressive-Like Behaviors and Neurotoxicity in Rats: Involvement of Oxidative Stress and Neuroinflammation. *Nutrients* **2016**, *8*, 243. [[CrossRef](#)] [[PubMed](#)]
68. Green, K.N.; Martinez-Coria, H.; Khashwji, H.; Hall, E.B.; Yurko-Mauro, K.A.; Ellis, L.; LaFerla, F.M. Dietary docosahexaenoic acid and docosapentaenoic acid ameliorate amyloid-beta and tau pathology via a mechanism involving presenilin 1 levels. *J. Neurosci.* **2007**, *27*, 4385–4395. [[CrossRef](#)] [[PubMed](#)]
69. Begum, G.; Yan, H.Q.; Li, L.; Singh, A.; Dixon, C.E.; Sun, D. Docosahexaenoic acid reduces ER stress and abnormal protein accumulation and improves neuronal function following traumatic brain injury. *J. Neurosci.* **2014**, *34*, 3743–3755. [[CrossRef](#)] [[PubMed](#)]
70. Plante, M.; Bailey, B.; Acworth, I. *Analysis of Lipids by RP-HPLC Using the Corona Analysis of Lipids by RP-HPLC Using the Corona Ultra*; ESA-A Dionex Company: Chelmsford, MA, USA, 2009.
71. Delobette, S.; Privat, A.; Maurice, T. In vitro aggregation facilitates beta-amyloid peptide-(25-35)-induced amnesia in the rat. *Eur. J. Pharmacol.* **1997**, *319*, 1–4. [[CrossRef](#)]



© 2017 by the authors. Licensee MDPI, Basel, Switzerland. This article is an open access article distributed under the terms and conditions of the Creative Commons Attribution (CC BY) license (<http://creativecommons.org/licenses/by/4.0/>).